International Journal of Solids and Structures 50 (2013) 3387–3398

Contents lists available at SciVerse ScienceDirect

International Journal of Solids and Structures

journal homepage: www.elsevier.com/locate/ijsolstr

The MFS for the Cauchy problem in two-dimensional steady-state linear thermoelasticity

Liviu Marin [a,b,*], Andreas Karageorghis [c]

[a] Institute of Solid Mechanics, Romanian Academy, 15 Constantin Mille, P.O. Box 1-863, 010141 Bucharest, Romania
[b] Centre for Continuum Mechanics, Faculty of Mathematics and Computer Science, University of Bucharest, 14 Academiei, 010014 Bucharest, Romania
[c] Department of Mathematics and Statistics, University of Cyprus, P.O. Box 20537, 1678 Nicosia, Cyprus

ARTICLE INFO

Article history:
Received 8 March 2013
Received in revised form 9 May 2013
Available online 18 June 2013

Keywords:
Linear thermoelasticity
Inverse problem
Cauchy problem
Method of fundamental solutions (MFS)
Method of particular solutions (MPS)
Regularization
L-curve method

ABSTRACT

We study the reconstruction of the missing thermal and mechanical fields on an inaccessible part of the boundary for two-dimensional linear isotropic thermoelastic materials from over-prescribed noisy (Cauchy) data on the remaining accessible boundary. This problem is solved with the method of fundamental solutions (MFS) together with the method of particular solutions (MPS) via the MFS-based particular solution for two-dimensional problems in uncoupled thermoelasticity developed in Marin and Karageorghis (2012a, 2013). The stabilisation/regularization of this inverse problem is achieved by using the Tikhonov regularization method (Tikhonov and Arsenin, 1986), whilst the optimal value of the regularization parameter is selected by employing Hansen's L-curve method (Hansen, 1998).

1. Introduction

Numerous stress analysis problems in engineering deal with structures which are simultaneously subject to thermal and mechanical loadings, i.e. thermoelastic loadings. This type of problems is encountered whenever a solid is subject to heating conditions that give rise to a temperature distribution throughout its volume. This temperature distribution produces thermal expansions in the object under consideration. In an isotropic material, at a uniform reference temperature, a small uniform increase in the temperature field can produce a pure volumetric expansion, provided that the solid body is not constrained against such a movement. This phenomenon can be expressed in terms of the so-called thermal strain, which is related to the difference between the temperature of the solid and the reference temperature through the coefficient of thermal expansion. It is important to mention that such a thermal expansion may also occur with no stresses present in the solid body, see e.g. Aliabadi (2002).

Mathematical problems of isotropic thermoelasticity have been the subject of numerous studies using various numerical methods such as the boundary element method (BEM) (Cheng et al., 2001; Henry and Banerjee, 1988; Kamiya et al., 1994; Rizzo and Shippy, 1977, 1979; Sladek and Sladek, 1983, 1984), the dual reciprocity BEM (DRBEM) (Partridge et al., 1992), the finite element method (FEM) (Dennis and Dulikravich, 1998, 1999), the moving least-squares method combined with the local boundary integral method (Sladek et al., 2001), etc. In the case of direct problems in thermoelasticity, the thermo-mechanical equilibrium equations have to be solved in a known geometry subject to known material constants, prescribed heat sources and/or body forces, and appropriate initial and boundary conditions for the temperature, normal heat flux, displacement and traction vectors. If at least one of the aforementioned conditions is unknown or incomplete then one needs to solve an *inverse problem*. A classical example of an inverse problem is the *Cauchy problem* in which the geometry of the solution domain, the thermo-mechanical material constants and the heat sources and body forces are all known, while both Dirichlet and Neumann conditions are prescribed on a part of the boundary and no information is provided on the remaining boundary. It is well known that Cauchy problems are generally ill-posed (Hadamard, 1923), in the sense that the existence, uniqueness and stability of their solutions are not always guaranteed. Consequently, a special numerical treatment of these problems is required.

The method of fundamental solutions (MFS) is a meshless boundary collocation method which is applicable to boundary value problems for which a fundamental solution of the operator in the governing equation is known. In spite of this restriction, the

* Corresponding author at: Institute of Solid Mechanics, Romanian Academy, 15 Constantin Mille, P.O. Box 1-863, 010141 Bucharest, Romania. Tel./fax: +40 (0)21 312 6736.
E-mail addresses: marin.liviu@gmail.com (L. Marin), andreask@ucy.ac.cy (A. Karageorghis).

0020-7683/$ - see front matter © 2013 Elsevier Ltd. All rights reserved.
http://dx.doi.org/10.1016/j.ijsolstr.2013.06.006

MFS has become very popular primarily because of the ease with which it can be implemented, in particular for the solution of problems in complex geometries. Since its introduction as a numerical method (Mathon and Johnston, 1977), it has been successfully applied to a large variety of physical problems, an account of which may be found in the survey papers by Fairweather and Karageorghis (1998); Fairweather et al. (2003); Golberg and Chen (1999); and Karageorghis et al. (2011). It is important to mention that the MFS belongs to the family of so-called *Trefftz methods* (Trefftz, 1926; Kita and Kamiya, 1995). Such methods have been used in several studies for the numerical solution of inverse problems related to solids subject to thermal or mechanical loads, see e.g. Ciałkowski and Frąckowiak (2002); Wróblewski and Zieliński (2006); Ciałkowski et al. (2007a,b); Karaś and Zieliński (2008); Liu (2008a,b); Ciałkowski and Grysa (2010); Karageorghis et al. (in press), etc.

Moreover, the MFS in conjunction with various regularization methods such as the Tikhonov regularization method and singular value decomposition, has been used increasingly over the last decade for the numerical solution of inverse problems. For example, the Cauchy problem associated with the heat conduction equation (Dong et al., 2007; Hon and Wei, 2004, 2005; Marin, 2008; Wei et al., 2007), linear elasticity (Marin, 2005a; Marin and Lesnic, 2004), steady-state heat conduction in functionally graded materials (Marin, 2005b), Helmholtz-type equations (Jin and Zheng, 2006; Marin, 2005c; Marin and Lesnic, 2005a), Stokes problems (Chen et al., 2005), the biharmonic equation (Marin and Lesnic, 2005b), etc. have all been successfully solved by the MFS. For a survey of applications of the MFS to inverse problems, we refer the reader to Karageorghis et al. (2011).

The MFS, in conjunction with the method of particular solutions (MPS) and the dual reciprocity method, was applied to direct problems in three-dimensional isotropic linear thermoelasticity in Karageorghis and Smyrlis (2007) and Tsai (2009), respectively. A comprehensive study of the application of the MFS–MPS to direct two-dimensional isotropic linear thermoelasticity problems was provided, apparently for the first time, in Marin and Karageorghis (2012a, 2013), while some preliminary results of this work may be found in Marin and Karageorghis (2012a).

In this study we investigate the numerical reconstruction of the unknown boundary thermoelastic fields on part of the boundary of the domain occupied by a two-dimensional isotropic linear thermoelastic solid from the knowledge of over-specified data on the remaining boundary (i.e. the Cauchy problem in planar isotropic linear thermoelasticity). This is achieved by combining the MFS–MPS algorithm developed in Marin and Karageorghis (2012a, 2013) with the Tikhonov regularization method (Tikhonov and Arsenin, 1986). The paper is organised as follows: In Section 2 we formulate mathematically the Cauchy problem under investigation. The proposed Tikhonov regularization algorithm is described in Section 3, while the MFS–MPS approach is presented in Section 4. The accuracy, convergence and stability of the proposed method are validated by analysing four numerical examples in Section 5. Finally, some conclusions are presented in Section 6.

2. Mathematical formulation

We consider an isotropic solid in a domain $\Omega \subset \mathbb{R}^2$, bounded by a curve $\partial\Omega$. The solid is characterised by the following material constants: the thermal conductivity, κ, the coefficient of linear thermal expansion, α_T, Poisson's ratio, ν, and the shear modulus, G.

In isotropic linear thermoelasticity, the strain tensor, $\boldsymbol{\epsilon} = [\epsilon_{ij}]_{1\leqslant i,j\leqslant 2}$, is related to the stress tensor, $\boldsymbol{\sigma} = [\sigma_{ij}]_{1\leqslant i,j\leqslant 2}$, by means of the constitutive law of isotropic linear thermoelasticity (Nowacki, 1986), namely

$$\boldsymbol{\epsilon}(\mathbf{x}) = \frac{1}{2G}\left[\boldsymbol{\sigma}(\mathbf{x}) - \frac{\overline{\nu}}{1+\overline{\nu}}\,\mathrm{tr}(\boldsymbol{\sigma}(\mathbf{x}))\mathbf{I}\right] + \overline{\alpha}_T \mathrm{T}(\mathbf{x})\mathbf{I}, \quad \mathbf{x} \in \overline{\Omega} = \Omega \cup \partial\Omega, \tag{1}$$

where $\mathbf{I} = [\delta_{ij}]_{1\leqslant i,j\leqslant 2}$, $\overline{\nu}$ is the equivalent Poisson's ratio ($\overline{\nu} = \nu$ for a plane strain state and $\overline{\nu} = \nu/(1+\nu)$ for a plane stress state) and $\overline{\alpha}_T$ is the equivalent coefficient of linear expansion ($\overline{\alpha}_T = \alpha_T$ and $\overline{\alpha}_T = \alpha_T(1+\nu)/(1+2\nu)$ for the plane strain and plane stress states, respectively). From (1) it follows that the shear strains are not affected by the temperature as the free thermal expansion does not produce any angular distortion in an isotropic material. Also, (1) may be written as

$$\boldsymbol{\sigma}(\mathbf{x}) = 2G\left[\boldsymbol{\epsilon}(\mathbf{x}) + \frac{\overline{\nu}}{1-2\overline{\nu}}\,\mathrm{tr}(\boldsymbol{\epsilon}(\mathbf{x}))\mathbf{I}\right] - \overline{\gamma}\mathrm{T}(\mathbf{x})\mathbf{I}, \quad \mathbf{x} \in \overline{\Omega}, \tag{2}$$

where the constant $\overline{\gamma}$ is related to the shear modulus, G, equivalent Poisson's ratio, $\overline{\nu}$, and equivalent coefficient of linear expansion, $\overline{\alpha}_T$, via the following formula

$$\overline{\gamma} = 2G\overline{\alpha}_T(1+\overline{\nu})/(1-2\overline{\nu}). \tag{3}$$

The kinematic relation

$$\boldsymbol{\epsilon}(\mathbf{x}) = \frac{1}{2}\left(\nabla\mathbf{u}(\mathbf{x}) + \nabla\mathbf{u}(\mathbf{x})^{\mathsf{T}}\right), \quad \mathbf{x} \in \overline{\Omega}, \tag{4}$$

combined with (2) yields

$$\boldsymbol{\sigma}(\mathbf{x}) = G\left[\left(\nabla\mathbf{u}(\mathbf{x}) + \nabla\mathbf{u}(\mathbf{x})^{\mathsf{T}}\right) + \frac{2\overline{\nu}}{1-2\overline{\nu}}(\nabla\cdot\mathbf{u}(\mathbf{x}))\mathbf{I}\right] - \overline{\gamma}\mathrm{T}(\mathbf{x})\mathbf{I}, \quad \mathbf{x} \in \overline{\Omega}. \tag{5}$$

By assuming the absence of body forces, the equilibrium equations of two-dimensional isotropic linear uncoupled thermoelasticity in terms of the displacement vector and the temperature (also known as the Navier–Lamé system of two-dimensional isotropic linear uncoupled thermoelasticity), become

$$-\nabla\cdot\boldsymbol{\sigma}(\mathbf{x}) \equiv \mathcal{L}\mathbf{u}(\mathbf{x}) + \overline{\gamma}\nabla\mathrm{T}(\mathbf{x}) = \mathbf{0}, \quad \mathbf{x} \in \Omega, \tag{6}$$

where $\mathcal{L} = (\mathcal{L}_1, \mathcal{L}_2)^{\mathsf{T}}$ is the partial differential operator associated with the Navier–Lamé system of isotropic linear elasticity, i.e.

$$\mathcal{L}\mathbf{u}(\mathbf{x}) \equiv -G\left[\nabla\cdot\left(\nabla\mathbf{u}(\mathbf{x}) + \nabla\mathbf{u}(\mathbf{x})^{\mathsf{T}}\right) + \frac{2\overline{\nu}}{1-2\overline{\nu}}\nabla(\nabla\cdot\mathbf{u}(\mathbf{x}))\right], \quad \mathbf{x} \in \Omega. \tag{7}$$

In the absence of heat sources, the governing heat conduction equation for two-dimensional steady-state isotropic linear uncoupled thermoelasticity becomes

$$-\nabla\cdot(\kappa\nabla\mathrm{T}(\mathbf{x})) = 0, \quad \mathbf{x} \in \Omega. \tag{8}$$

Further, we let $\mathbf{n}(\mathbf{x})$ be the outward unit normal vector to $\partial\Omega$, $\mathrm{q}(\mathbf{x})$ be the normal heat flux at a point $\mathbf{x} \in \partial\Omega$ defined by

$$\mathrm{q}(\mathbf{x}) \equiv -(\kappa\nabla\mathrm{T}(\mathbf{x}))\cdot\mathbf{n}(\mathbf{x}), \quad \mathbf{x} \in \partial\Omega \tag{9}$$

and $\mathbf{t}(\mathbf{x})$ be the traction vector at $\mathbf{x} \in \partial\Omega$ given by

$$\mathbf{t}(\mathbf{x}) \equiv \boldsymbol{\sigma}(\mathbf{x})\,\mathbf{n}(\mathbf{x}), \quad \mathbf{x} \in \partial\Omega. \tag{10}$$

In the direct (forward) formulation of the two-dimensional uncoupled thermoelasticity problem, the temperature and normal heat flux are prescribed on the boundaries Γ_T and Γ_q, respectively, where $\Gamma_T \cup \Gamma_q = \partial\Omega$ and $\Gamma_T \cap \Gamma_q = \varnothing$, while the displacement and traction vectors are given on the boundaries $\Gamma_{\mathbf{u}}$ and $\Gamma_{\mathbf{t}}$, respectively, where $\Gamma_{\mathbf{u}} \cup \Gamma_{\mathbf{t}} = \partial\Omega$ and $\Gamma_{\mathbf{u}} \cap \Gamma_{\mathbf{t}} = \varnothing$. However, in many practical situations, only a part of the boundary, say $\Gamma_1 := \Gamma_T = \Gamma_q = \Gamma_{\mathbf{u}} = \Gamma_{\mathbf{t}} \subset \partial\Omega$, is accessible for measurements, while the remaining boundary, $\Gamma_2 = \partial\Omega \setminus \overline{\Gamma}_1$, is inaccessible and hence no measurements are available on it. In the sequel, we

assume that the temperature and normal heat flux, as well as the displacement and traction vectors can be measured on $\Gamma_1 \subset \partial\Omega$, while the remaining boundary, Γ_2, is inaccessible and no boundary data are available on it. This problem is a *Cauchy problem* and consists of Eqs. (6) and (8), and the thermal and mechanical boundary conditions

$$\mathrm{T}(\mathbf{x}) = \widetilde{\mathrm{T}}(\mathbf{x}) \quad \text{and} \quad \mathrm{q}(\mathbf{x}) = \widetilde{\mathrm{q}}(\mathbf{x}), \quad \mathbf{x} \in \Gamma_1 \tag{11a}$$

and

$$\mathbf{u}(\mathbf{x}) = \widetilde{\mathbf{u}}(\mathbf{x}) \quad \text{and} \quad \mathbf{t}(\mathbf{x}) = \widetilde{\mathbf{t}}(\mathbf{x}), \quad \mathbf{x} \in \Gamma_1, \tag{11b}$$

respectively, where $\widetilde{\mathrm{T}}, \widetilde{\mathrm{q}}, \widetilde{\mathbf{u}}$ and $\widetilde{\mathbf{t}}$ are given. The Cauchy problem (6), (8) and (11) is considerably more difficult to solve both analytically and numerically than direct problems since its solution does not satisfy the general conditions of well-posedness, see e.g. Hadamard (1923).

3. Solution algorithm

We consider the solution of the inverse Cauchy problem given by Eqs. (6), (8) and (11), using a combined MFS–MPS approach as originally proposed by Marin and Karageorghis (2012a, 2013), together with the Tikhonov regularization method (Tikhonov and Arsenin, 1986). The Cauchy problem for the heat conduction equation given by Eqs. (8) and (11b) is first solved by applying the MFS in conjunction with the Tikhonov regularization method. Next, we derive a particular solution of the equilibrium equations of (6) according to the method developed by Marin and Karageorghis (2012a, 2013). Finally, we apply the MFS to the resulting Cauchy problem corresponding to the homogeneous equilibrium equations for a two-dimensional isotropic linear elastic material and solve this inverse problem using the Tikhonov regularization method.

The numerical procedure described above may be summarised as follows:

Step 1. Solve the thermal Cauchy problem (8) and (11a) with the Tikhonov regularization method to determine the unknown boundary temperature $\mathrm{T}|_{\Gamma_2}$ and flux $\mathrm{q}|_{\Gamma_2}$, as well as the temperature distribution in the domain $\mathrm{T}|_{\Omega}$.

Step 2. Solve the mechanical Cauchy problem (6) and (11b):

Step 2.1. Determine a particular solution $\mathbf{u}^{(\mathrm{P})}$ of the non-homogeneous equilibrium equation (6) in Ω, as well as the corresponding particular strain tensor

$$\boldsymbol{\epsilon}^{(\mathrm{P})}(\mathbf{x}) = \frac{1}{2}\left(\nabla\mathbf{u}^{(\mathrm{P})}(\mathbf{x}) + \nabla\mathbf{u}^{(\mathrm{P})}(\mathbf{x})^{\mathrm{T}}\right), \quad \mathbf{x} \in \overline{\Omega}, \tag{12a}$$

stress tensor

$$\boldsymbol{\sigma}^{(\mathrm{P})}(\mathbf{x}) = 2G\left[\boldsymbol{\epsilon}^{(\mathrm{P})}(\mathbf{x}) + \frac{\overline{\nu}}{1-2\overline{\nu}}\,\mathrm{tr}\left(\boldsymbol{\epsilon}^{(\mathrm{P})}(\mathbf{x})\right)\mathbf{I}\right], \quad \mathbf{x} \in \overline{\Omega} \tag{12b}$$

and traction vector

$$\mathbf{t}^{(\mathrm{P})}(\mathbf{x}) = \boldsymbol{\sigma}^{(\mathrm{P})}(\mathbf{x})\,\mathbf{n}(\mathbf{x}), \quad \mathbf{x} \in \partial\Omega. \tag{12c}$$

It should be noted that $\mathbf{u}^{(\mathrm{P})}$ depends on the solution of the thermal Cauchy problem (8) and (11a); consequently, the same remark holds for $\boldsymbol{\epsilon}^{(\mathrm{P})}, \boldsymbol{\sigma}^{(\mathrm{P})}$ and $\mathbf{t}^{(\mathrm{P})}$.

Step 2.2. Solve the Cauchy problem corresponding to the homogeneous equilibrium equations, i.e.

$$\mathcal{L}\mathbf{u}^{(\mathrm{H})}(\mathbf{x}) = \mathbf{0}, \quad \mathbf{x} \in \Omega, \tag{13a}$$

$$\mathbf{u}^{(\mathrm{H})}(\mathbf{x}) = \widetilde{\mathbf{u}}(\mathbf{x}) - \mathbf{u}^{(\mathrm{P})}(\mathbf{x}), \quad \mathbf{x} \in \Gamma_1, \tag{13b}$$

$$\mathbf{t}^{(\mathrm{H})}(\mathbf{x}) = \widetilde{\mathbf{t}}(\mathbf{x}) - \left[\mathbf{t}^{(\mathrm{P})}(\mathbf{x}) - \overline{\gamma}\mathrm{T}(\mathbf{x})\,\mathbf{n}(\mathbf{x})\right], \quad \mathbf{x} \in \Gamma_1, \tag{13c}$$

using the Tikhonov regularization method to determine $\mathbf{u}^{(\mathrm{H})}|_{\Gamma_2}, \mathbf{t}^{(\mathrm{H})}|_{\Gamma_2}$ and $\mathbf{u}^{(\mathrm{H})}|_{\Omega}$.

Step 2.3. On applying the superposition principle, determine the unknown boundary displacement $\mathbf{u}|_{\Gamma_2} = \mathbf{u}^{(\mathrm{H})}|_{\Gamma_2} + \mathbf{u}^{(\mathrm{P})}|_{\Gamma_2}$ and boundary traction $\mathbf{t}|_{\Gamma_2} = \mathbf{t}^{(\mathrm{H})}|_{\Gamma_2} + \left(\mathbf{t}^{(\mathrm{P})} - \overline{\gamma}\mathrm{T}\mathbf{n}\right)|_{\Gamma_2}$, as well as the mechanical fields inside the domain, namely $\mathbf{u}|_{\Omega} = \mathbf{u}^{(\mathrm{H})}|_{\Omega} + \mathbf{u}^{(\mathrm{P})}|_{\Omega}$, $\boldsymbol{\epsilon}|_{\Omega} = \boldsymbol{\epsilon}^{(\mathrm{H})}|_{\Omega} + \boldsymbol{\epsilon}^{(\mathrm{P})}|_{\Omega}$ and $\boldsymbol{\sigma}|_{\Omega} = \boldsymbol{\sigma}^{(\mathrm{H})}|_{\Omega} + \left(\boldsymbol{\sigma}^{(\mathrm{P})} - \overline{\gamma}\mathrm{T}\mathbf{I}\right)|_{\Omega}$.

The proposed algorithm relies on the existence of a particular solution of the non-homogeneous equilibrium equation (6) which is justified by the following result, see e.g. Marin and Karageorghis (2012a, 2013):

Proposition 1. *Let $\Omega \subset \mathbb{R}^2$ be a domain occupied by an isotropic solid characterised by the constant thermal conductivity, κ, the coefficient of linear thermal expansion, α_{T}, Poisson's ratio, ν, and the shear modulus, G, respectively, and let $\overline{\gamma}$ be given by Eq. (3).*

Then for any set $X_{\mathrm{K}} = \{\mathbf{x}^{(k)}\}_{k=1}^{\mathrm{K}} \subset \mathbb{R}^2 \setminus \overline{\Omega}$, $\mathrm{K} \in \mathbb{Z}_+$, the temperature field

$$\mathrm{T}^{(\mathrm{P})}(\mathbf{x}) = \sum_{k=1}^{\mathrm{K}} \mathrm{T}_k \log\|\mathbf{x} - \mathbf{x}^{(k)}\|, \quad \mathbf{x} \in \overline{\Omega}, \tag{14a}$$

where $\mathrm{T}_k \in \mathbb{R}$, $1 \leqslant k \leqslant \mathrm{K}$, and the displacement vector

$$\mathbf{u}^{(\mathrm{P})}(\mathbf{x}) = \frac{\overline{\gamma}}{4G}\left(\frac{1-2\overline{\nu}}{1-\overline{\nu}}\right)\sum_{k=1}^{\mathrm{K}} \mathrm{T}_k\left(\mathbf{x} - \mathbf{x}^{(k)}\right)\log\|\mathbf{x} - \mathbf{x}^{(k)}\|, \quad \mathbf{x} \in \overline{\Omega}, \tag{14b}$$

represent a particular solution $\left(\mathrm{T}^{(\mathrm{P})}, \mathbf{u}^{(\mathrm{P})}\right) \in \left(\mathrm{C}^{\infty}\left(\overline{\Omega}\right)\right)^3$ of the governing equations of two-dimensional isotropic linear thermoelasticity (6) and (8).

As a direct consequence of Proposition 1, the expressions for the corresponding particular strain tensor, $\boldsymbol{\epsilon}^{(\mathrm{P})}$, stress tensor $\boldsymbol{\sigma}^{(\mathrm{P})}$, and traction vector $\mathbf{t}^{(\mathrm{P})}$, are obtained by substituting the particular displacement vector given by (14b) into Eqs. (12a)–(12c), respectively, i.e.

$$\boldsymbol{\epsilon}^{(\mathrm{P})}(\mathbf{x}) = \frac{\overline{\gamma}}{4G}\left(\frac{1-2\overline{\nu}}{1-\overline{\nu}}\right)\sum_{k=1}^{\mathrm{K}} \mathrm{T}_k\left[\log\|\mathbf{x}-\mathbf{x}^{(k)}\|\mathbf{I} + \frac{\mathbf{x}-\mathbf{x}^{(k)}}{\|\mathbf{x}-\mathbf{x}^{(k)}\|} \otimes \frac{\mathbf{x}-\mathbf{x}^{(k)}}{\|\mathbf{x}-\mathbf{x}^{(k)}\|}\right], \quad \mathbf{x} \in \overline{\Omega}, \tag{15a}$$

$$\boldsymbol{\sigma}^{(\mathrm{P})}(\mathbf{x}) = \frac{\overline{\gamma}}{2}\left(\frac{1-2\overline{\nu}}{1-\overline{\nu}}\right)\sum_{k=1}^{\mathrm{K}} \mathrm{T}_k\left[\frac{1}{1-2\overline{\nu}}\left(\log\|\mathbf{x}-\mathbf{x}^{(k)}\| + \overline{\nu}\right)\mathbf{I} + \frac{\mathbf{x}-\mathbf{x}^{(k)}}{\|\mathbf{x}-\mathbf{x}^{(k)}\|} \otimes \frac{\mathbf{x}-\mathbf{x}^{(k)}}{\|\mathbf{x}-\mathbf{x}^{(k)}\|}\right], \quad \mathbf{x} \in \overline{\Omega} \tag{15b}$$

and

$$\mathbf{t}^{(\mathrm{P})}(\mathbf{x}) = \frac{\overline{\gamma}}{2}\left(\frac{1-2\overline{\nu}}{1-\overline{\nu}}\right)\sum_{k=1}^{\mathrm{K}} \mathrm{T}_k\left[\frac{1}{1-2\overline{\nu}}\left(\log\|\mathbf{x}-\mathbf{x}^{(k)}\| + \overline{\nu}\right)\mathbf{n}(\mathbf{x}) + \frac{\left(\mathbf{x}-\mathbf{x}^{(k)}\right)\cdot\mathbf{n}(\mathbf{x})}{\|\mathbf{x}-\mathbf{x}^{(k)}\|^2}\left(\mathbf{x}-\mathbf{x}^{(k)}\right)\right], \quad \mathbf{x} \in \partial\Omega. \tag{15c}$$

Clearly, as explained in Marin and Karageorghis (2013), analytical solutions can be easily constructed from Proposition 1. This is achieved by simply setting $\mathrm{K} \in \mathbb{Z}_+$ and choosing a set of points $X_{\mathrm{K}} = \{\mathbf{x}^{(k)}\}_{k=1}^{\mathrm{K}} \subset \mathbb{R}^2 \setminus \overline{\Omega}$, as well as constants $\mathrm{T}_k \in \mathbb{R}$, $1 \leqslant k \leqslant \mathrm{K}$. The corresponding analytical solution of the governing equations (6) and (8) is given by Eqs. (14a) and (14b), respectively.

4. The method of fundamental solutions

Step 1. The fundamental solution of the heat balance equation (8) for two-dimensional steady-state heat conduction in an isotropic homogeneous medium (Fairweather and Karageorghis, 1998) is

$$\mathrm{F}(\mathbf{x}, \boldsymbol{\xi}) = -\frac{1}{2\pi\kappa}\log\|\mathbf{x} - \boldsymbol{\xi}\|, \quad \mathbf{x} \in \overline{\Omega}, \tag{16}$$

where $\mathbf{x} = (x_1, x_2)$ is a collocation point and $\boldsymbol{\xi} = (\xi_1, \xi_2) \in \mathbb{R}^2 \setminus \overline{\Omega}$ is a singularity or source point. In the MFS, the temperature is approximated by a linear combination of fundamental solutions with respect to N_s^L singularities, $\{\boldsymbol{\xi}^{(n)}\}_{n=1}^{N_s^L}$, in the form

$$T(\mathbf{x}) \approx T_{N_s^L}(\mathbf{c}^{(1)}, \boldsymbol{\xi}; \mathbf{x}) = \sum_{n=1}^{N_s^L} c_n^{(1)} F(\mathbf{x}, \boldsymbol{\xi}^{(n)}), \quad \mathbf{x} \in \overline{\Omega}, \tag{17}$$

where $\mathbf{c}^{(1)} = \left[c_1^{(1)}, \ldots, c_{N_s^L}^{(1)}\right]^T \in \mathbb{R}^{N_s^L}$ and $\boldsymbol{\xi} \in \mathbb{R}^{2N_s^L}$ is a vector containing the coordinates of the singularities. From Eqs. (9) and (16) it follows that the normal heat flux, through a curve defined by the outward unit normal vector $\mathbf{n}(\mathbf{x})$, can be approximated on the boundary $\partial\Omega$ by

$$q(\mathbf{x}) \approx q_{N_s^L}(\mathbf{c}^{(1)}, \boldsymbol{\xi}; \mathbf{x}) = -\sum_{n=1}^{N_s^L} c_n^{(1)} \left[\kappa \nabla_{\mathbf{x}} F(\mathbf{x}, \boldsymbol{\xi}^{(n)}) \cdot \mathbf{n}(\mathbf{x})\right], \quad \mathbf{x} \in \partial\Omega. \tag{18}$$

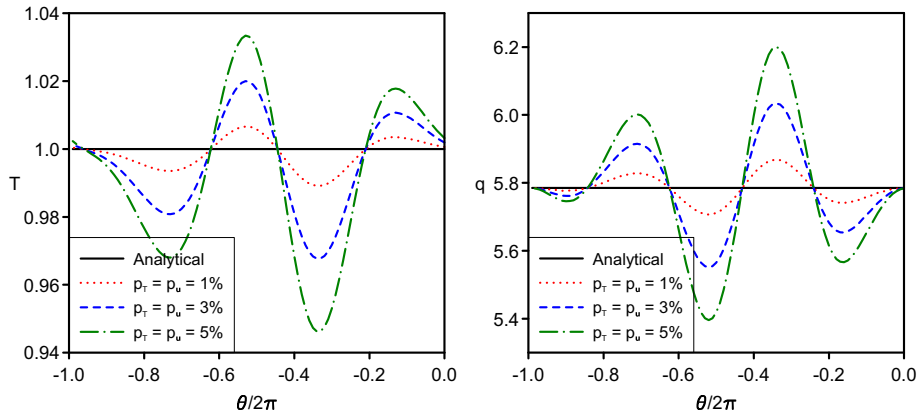

(a) Example 1: $T|_{\Gamma_2}$ (b) Example 1: $q|_{\Gamma_2}$

Fig. 1. The analytical and numerical (a) temperatures $T|_{\Gamma_2}$ and (b) normal heat fluxes $q|_{\Gamma_2}$, obtained using various levels of noise added in $T|_{\Gamma_1}$ and $u|_{\Gamma_1}$, for Example 1.

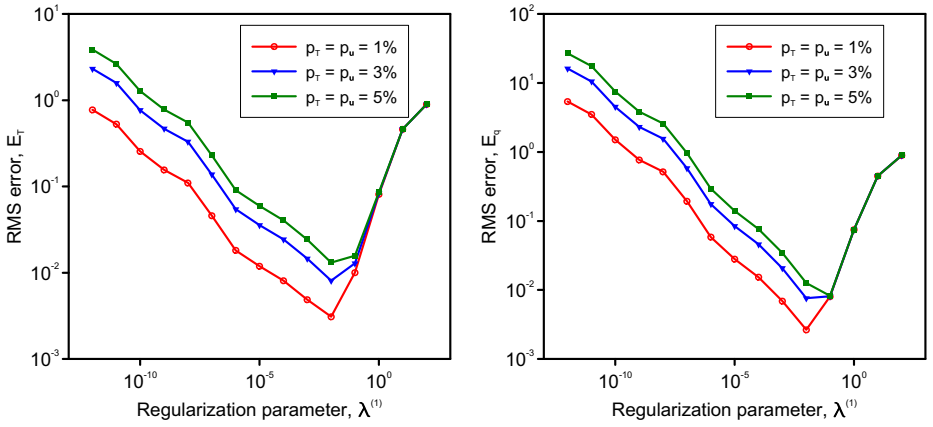

(a) Example 1: Err_T (b) Example 1: Err_q

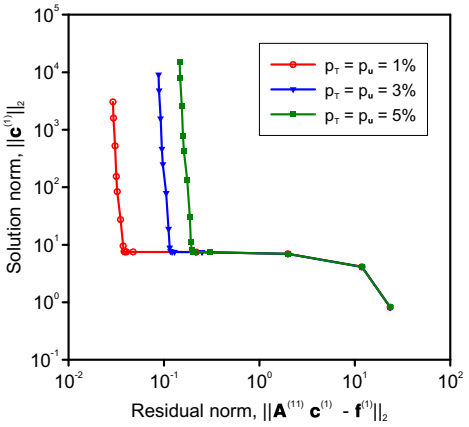

(c) Example 1: L-curves

Fig. 2. The RMS errors (a) Err_T and (b) Err_T, as functions of the regularization parameter, $\lambda^{(1)}$, and (c) the corresponding L-curves, obtained using various levels of noise added in $T|_{\Gamma_1}$ and $u|_{\Gamma_1}$, for the thermal Cauchy problem associated with Example 1.

Next, we select N_c^L MFS collocation points, $\{\mathbf{x}^{(n)}\}_{n=1}^{N_c^L}$, on the boundary Γ_1 and collocate the Cauchy thermal boundary conditions (11a) to obtain the following system of linear equations for the unknown coefficients $\mathbf{c}^{(1)} \in \mathbb{R}^{N_s^L}$:

$$\mathbf{A}^{(11)}\,\mathbf{c}^{(1)} = \mathbf{f}^{(1)}, \tag{19}$$

where $\mathbf{A}^{(11)} \in \mathbb{R}^{2N_c^L \times N_s^L}$ is the corresponding MFS matrix whose elements are calculated from Eqs. (17) and (18), respectively, while $\mathbf{f}^{(1)} \in \mathbb{R}^{2N_c^L}$ contains the corresponding discretised Cauchy data (11a).

Step 2.1. The MFS approximation for the particular solution to the non-homogeneous equilibrium equations (6) in $\mathbb{R}^2$ is (Marin and Karageorghis, 2012a, 2013)

$$\mathbf{u}^{(\mathrm{P})}(\mathbf{y}) \approx \mathbf{u}^{(\mathrm{P})}_{N_s^L}(\mathbf{c}^{(1)}, \xi; \mathbf{y}) = -\frac{\overline{\gamma}}{8\pi\kappa G}\left(\frac{1-2\overline{\nu}}{1-\overline{\nu}}\right)\sum_{n=1}^{N_s^L} c_n^{(1)} \times \left(\mathbf{y}-\xi^{(n)}\right)\log\|\mathbf{y}-\xi^{(n)}\|,\ \mathbf{y} \in \mathbb{R}^2 \setminus \bigcup_{n=1}^{N_s^L}\{\xi^{(n)}\}, \tag{20}$$

and hence the corresponding approximation for the particular traction vector on the boundary $\partial\Omega$ is obtained as

$$\mathbf{t}^{(\mathrm{P})}(\mathbf{y}) \approx \mathbf{t}^{(\mathrm{P})}_{N_s^L}(\mathbf{c}^{(1)}, \xi; \mathbf{y}) = -\frac{\overline{\gamma}}{4\pi\kappa}\left(\frac{1-2\overline{\nu}}{1-\overline{\nu}}\right)\sum_{n=1}^{N_s^L} c_n^{(1)} \times \left[\frac{1}{1-2\overline{\nu}}\left(\log\|\mathbf{y}-\xi^{(n)}\| + \overline{\nu}\right)\mathbf{n}(\mathbf{y}) + \frac{(\mathbf{y}-\xi^{(n)})\cdot\mathbf{n}(\mathbf{y})}{\|\mathbf{y}-\xi^{(n)}\|^2}(\mathbf{y}-\xi^{(n)})\right],\ \mathbf{y} \in \partial\Omega. \tag{21}$$

Consequently, the term $\left(\mathbf{t}^{(\mathrm{P})} - \overline{\gamma}\mathrm{T}\mathbf{n}\right)$ is approximated on $\partial\Omega$ by

$$\mathbf{t}^{(\mathrm{P})}(\mathbf{y}) - \overline{\gamma}\,\mathrm{T}(\mathbf{y})\,\mathbf{n}(\mathbf{y}) \approx \mathbf{t}^{(\mathrm{P})}_{N_s^L}(\mathbf{c}^{(1)}, \xi; \mathbf{y}) - \overline{\gamma}\,\mathrm{T}_{N_s^L}(\mathbf{y})\,\mathbf{n}(\mathbf{y}) = \frac{\overline{\gamma}}{4\pi\kappa}\left(\frac{1-2\overline{\nu}}{1-\overline{\nu}}\right) \times \sum_{n=1}^{N_s^L} c_n^{(1)}\left[\left(\log\|\mathbf{y}-\xi^{(n)}\| - \frac{\overline{\nu}}{1-2\overline{\nu}}\right)\mathbf{n}(\mathbf{y}) + \frac{(\mathbf{y}-\xi^{(n)})\cdot\mathbf{n}(\mathbf{y})}{\|\mathbf{y}-\xi^{(n)}\|^2}(\mathbf{y}-\xi^{(n)})\right],\quad \mathbf{y} \in \partial\Omega. \tag{22}$$

Note that once the coefficients, $\mathbf{c}^{(1)} \in \mathbb{R}^{N_s^L}$, corresponding to the thermal Cauchy problem (8) and (11a) are retrieved by solving Eq. (19) with the Tikhonov regularization method, the particular solutions for the boundary displacement and traction vectors on Γ_1 are expressed from Eqs. (20) and (21), respectively.

Step 2.2. The fundamental solution matrix $\mathbf{U} = \left[\mathrm{U}_{ij}\right]_{1\leqslant i,j\leqslant 2}$, for the displacement vector in the Navier-Lamé system is given by Aliabadi (2002)

$$\mathrm{U}_{ij}(\mathbf{y},\boldsymbol{\eta}) = \frac{1}{8\pi G(1-\overline{\nu})}\left[-(3-4\overline{\nu})\log\|\mathbf{y}-\boldsymbol{\eta}\|\,\delta_{ij} + \frac{\mathrm{y}_i-\eta_i}{\|\mathbf{x}-\boldsymbol{\eta}\|}\frac{\mathrm{y}_j-\eta_j}{\|\mathbf{x}-\boldsymbol{\eta}\|}\right],\quad \mathbf{y} \in \overline{\Omega},\ i,j=1,2, \tag{23}$$

where $\mathbf{y} = (\mathrm{y}_1, \mathrm{y}_2) \in \overline{\Omega}$ is a collocation point and $\boldsymbol{\eta} = (\eta_1, \eta_2) \in \mathbb{R}^2 \setminus \overline{\Omega}$ is a singularity. By differentiating Eq. (23) with respect to y_k, $k = 1, 2$, one obtains the derivatives of the fundamental solution for the displacement vector, denoted by $\partial_{\mathrm{y}_k}\mathrm{U}_{ij}(\mathbf{y},\boldsymbol{\eta})$, where $\partial_{\mathrm{y}_k} \equiv \partial/\partial\mathrm{y}_k$. The fundamental solution matrix $\mathbf{T} = \left[\mathrm{T}_{ij}\right]_{1\leqslant i,j\leqslant 2}$, for the traction vector in the case of two-dimensional isotropic linear elasticity is then obtained by combining Eq. (23) with

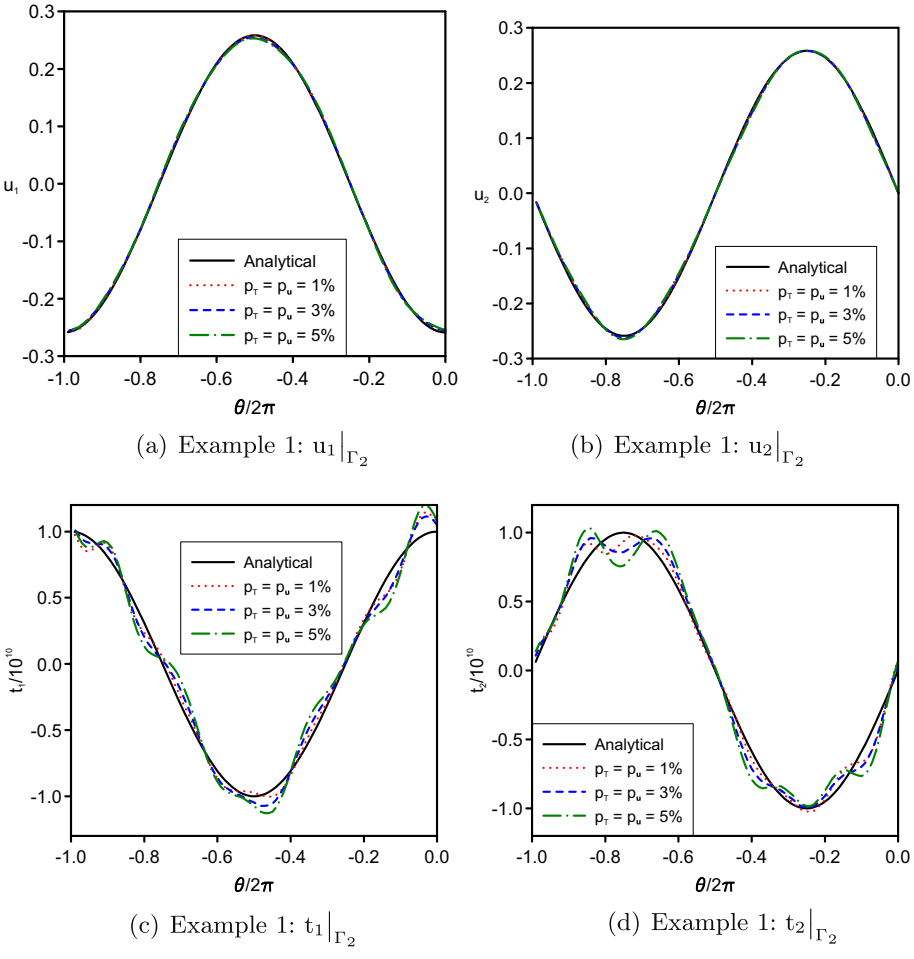

(a) Example 1: $\mathrm{u}_1\big|_{\Gamma_2}$ (b) Example 1: $\mathrm{u}_2\big|_{\Gamma_2}$

(c) Example 1: $\mathrm{t}_1\big|_{\Gamma_2}$ (d) Example 1: $\mathrm{t}_2\big|_{\Gamma_2}$

Fig. 3. The analytical and numerical displacements (a) $\mathrm{u}_1|_{\Gamma_2}$ and (b) $\mathrm{u}_2|_{\Gamma_2}$, and tractions (c) $\mathrm{t}_1|_{\Gamma_2}$ and (d) $\mathrm{t}_2|_{\Gamma_2}$, obtained using various levels of noise added in $\mathrm{T}|_{\Gamma_1}$ and $\mathrm{u}|_{\Gamma_1}$, for Example 1.

the definition of the traction vector and Hooke's constitutive law of isotropic linear elasticity (Aliabadi, 2002), namely

$$\mathsf{T}_{1k}(\mathbf{y},\boldsymbol{\eta}) = \frac{2G}{1-2\overline{\nu}}\left[(1-\overline{\nu})\partial_{y_1}\mathsf{U}_{1k}(\mathbf{y},\boldsymbol{\eta}) + \overline{\nu}\partial_{y_2}\mathsf{U}_{2k}(\mathbf{y},\boldsymbol{\eta})\right]\mathrm{n}_1(\mathbf{y}) + G\left[\partial_{y_2}\mathsf{U}_{1k}(\mathbf{y},\boldsymbol{\eta}) + \partial_{y_1}\mathsf{U}_{2k}(\mathbf{y},\boldsymbol{\eta})\right]\mathrm{n}_2(\mathbf{y}), \quad \mathbf{y}\in\partial\Omega,\ k=1,2, \tag{24a}$$

and

$$\mathsf{T}_{2k}(\mathbf{y},\boldsymbol{\eta}) = G\left[\partial_{y_2}\mathsf{U}_{1k}(\mathbf{y},\boldsymbol{\eta}) + \partial_{y_1}\mathsf{U}_{2k}(\mathbf{y},\boldsymbol{\eta})\right]\mathrm{n}_1(\mathbf{y}) + \frac{2G}{1-2\overline{\nu}}\left[\overline{\nu}\,\partial_{y_1}\mathsf{U}_{1k}(\mathbf{y},\boldsymbol{\eta}) + (1-\overline{\nu})\,\partial_{y_2}\mathsf{U}_{2k}(\mathbf{y},\boldsymbol{\eta})\right]\mathrm{n}_2(\mathbf{y}), \quad \mathbf{y}\in\partial\Omega,\ k=1,2. \tag{24b}$$

As for the thermal Cauchy problem, we consider $\mathrm{N}_s^{\mathrm{E}}$ singularities, $\{\boldsymbol{\eta}^{(n)}\}_{n=1}^{\mathrm{N}_s^{\mathrm{E}}}$, and approximate the displacement vector, $\mathbf{u}^{(\mathrm{H})}$, associated with the homogeneous equilibrium equation (13a) in the solution domain by a linear combination of the displacement fundamental solutions (23) with respect to these singularities, i.e.

$$\mathbf{u}^{(\mathrm{H})}(\mathbf{y}) \approx \mathbf{u}^{(\mathrm{H})}_{\mathrm{N}_s^{\mathrm{E}}}(\mathbf{c}^{(2)},\boldsymbol{\eta};\mathbf{y}) = \sum_{n=1}^{\mathrm{N}_s^{\mathrm{E}}}\mathbf{U}(\mathbf{y},\boldsymbol{\eta}^{(n)})\,\mathbf{c}_n^{(2)}, \quad \mathbf{y}\in\overline{\Omega}, \tag{25}$$

where $\mathbf{c}_n^{(2)} = \left[c_{n;1}^{(2)}, c_{n;2}^{(2)}\right]^{\mathsf{T}} \in \mathbb{R}^2,\ n=1,\ldots,\mathrm{N}_s^{\mathrm{E}},\ \mathbf{c}^{(2)} = \left[\left(\mathbf{c}_1^{(2)}\right)^{\mathsf{T}}, \left(\mathbf{c}_2^{(2)}\right)^{\mathsf{T}}\ldots, \left(\mathbf{c}_{\mathrm{N}_s^{\mathrm{E}}}^{(2)}\right)^{\mathsf{T}}\right]^{\mathsf{T}} \in \mathbb{R}^{2\mathrm{N}_s^{\mathrm{E}}}$ and $\boldsymbol{\eta}\in\mathbb{R}^{2\mathrm{N}_s^{\mathrm{E}}}$ is a vector containing the coordinates of the singularities $\{\boldsymbol{\eta}^{(n)}\}_{n=1}^{\mathrm{N}_s^{\mathrm{E}}}$. In a similar manner, the traction vector, $\mathbf{t}^{(\mathrm{H})}$, associated with the homogeneous equilibrium equation (13a) is approximated by a linear combination of the traction fundamental solutions (24a) and (24b), namely

$$\mathbf{t}^{(\mathrm{H})}(\mathbf{y}) \approx \mathbf{t}^{(\mathrm{H})}_{\mathrm{N}_s^{\mathrm{E}}}(\mathbf{c}^{(2)},\boldsymbol{\eta};\mathbf{y}) = \sum_{n=1}^{\mathrm{N}_s^{\mathrm{E}}}\mathbf{T}(\mathbf{y},\boldsymbol{\eta}^{(n)})\,\mathbf{c}_n^{(2)}, \quad \mathbf{y}\in\partial\Omega. \tag{26}$$

By collocating the boundary conditions (13b) and (13c) at the points $\{\mathbf{y}^{(n)}\}_{n=1}^{\mathrm{N}_c^{\mathrm{E}}}$ on the boundary Γ_1, one obtains the following system of linear equations for the unknown coefficients $\mathbf{c}^{(2)}\in\mathbb{R}^{2\mathrm{N}_s^{\mathrm{E}}}$:

$$\mathbf{A}^{(22)}\,\mathbf{c}^{(2)} = \mathbf{f}^{(2)} - \mathbf{A}^{(21)}\,\mathbf{c}^{(1)}, \tag{27}$$

where $\mathbf{A}^{(22)}\in\mathbb{R}^{4\mathrm{N}_c^{\mathrm{E}}\times 2\mathrm{N}_s^{\mathrm{E}}}$ is the corresponding MFS matrix whose elements are calculated from Eqs. (25) and (26), respectively, $\mathbf{f}^{(2)}\in\mathbb{R}^{4\mathrm{N}_c^{\mathrm{E}}}$ is the right-hand side vector containing the corresponding discretised Cauchy data (11b) and the elements of the matrix $\mathbf{A}^{(21)}\in\mathbb{R}^{4\mathrm{N}_c^{\mathrm{E}}\times\mathrm{N}_s^{\mathrm{L}}}$ are determined from those of the MFS matrices that approximate $\mathbf{u}^{(\mathrm{P})}(\mathbf{y}^{(n)})$ and $(\mathbf{t}^{(\mathrm{P})} - \overline{\gamma}\mathsf{T}\mathbf{n})(\mathbf{y}^{(n)})$, $n=1,\ldots,\mathrm{N}_c^{\mathrm{E}}$, according to Eqs. (13a), (13b), (20) and (22).

Step 2.3. Having determined the coefficients $\mathbf{c}^{(2)}\in\mathbb{R}^{2\mathrm{N}_s^{\mathrm{E}}}$, the approximations of the boundary displacement, $\mathbf{u}|_{\Gamma_t}$, and traction vectors, $\mathbf{t}|_{\Gamma_u}$, are obtained from the superposition principle and Eqs. (20), (22), (25) and (26).

4.1. Tikhonov regularization method

In order to uniquely determine the solutions $\mathbf{c}^{(1)}\in\mathbb{R}^{\mathrm{N}_s^{\mathrm{L}}}$ and $\mathbf{c}^{(2)}\in\mathbb{R}^{2\mathrm{N}_s^{\mathrm{E}}}$, the corresponding numbers of boundary collocation

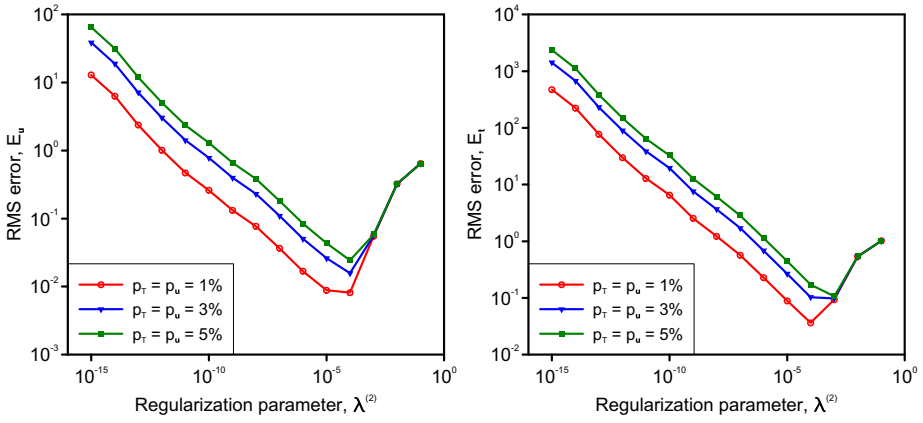

(a) Example 1: $\mathrm{Err}_{\mathbf{u}}$ (b) Example 1: $\mathrm{Err}_{\mathbf{t}}$

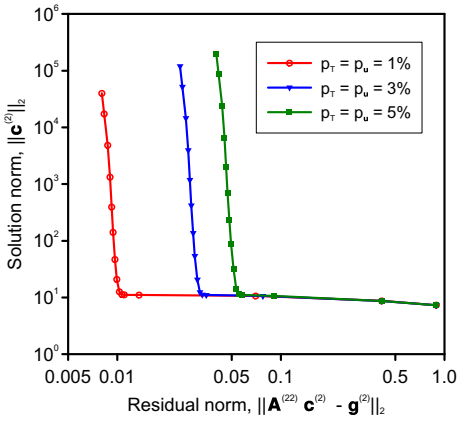

(c) Example 1: L-curves

Fig. 4. The RMS errors (a) Err_u and (b) Err_t, as functions of the regularization parameter, $\lambda^{(2)}$, and (c) the corresponding L-curves, obtained using various levels of noise added in $\mathsf{T}|_{\Gamma_1}$ and $u|_{\Gamma_1}$, for the mechanical Cauchy problem associated with Example 1.

points and singularities must satisfy the inequalities $N_s^L \leqslant 2N_c^L$ and $N_s^E \leqslant 2N_c^E$, respectively. These ill-conditioned systems cannot be solved by direct methods, such as the least-squares method, since such an approach would produce a highly unstable solution in the case of noisy Cauchy data on Γ_1. Therefore, systems (19) and (27) are solved, in a stable manner, by employing the Tikhonov regularization method (Tikhonov and Arsenin, 1986).

The Tikhonov regularized solution, $\mathbf{c}^{(1)}_{\lambda^{(1)}}$, of system (19) is sought as the minimum of the Tikhonov regularization functional given by

$$\mathcal{F}^{(1)}_{\lambda^{(1)}}(\cdot) : \mathbb{R}^{N_s^L} \longrightarrow [0,\infty),$$
$$\mathcal{F}^{(1)}_{\lambda^{(1)}}(\mathbf{c}^{(1)}) = \|\mathbf{A}^{(11)}\mathbf{c}^{(1)} - \mathbf{f}^{(1)}\|^2 + \lambda^{(1)}\|\mathbf{c}^{(1)}\|^2, \tag{28}$$

where $\lambda^{(1)} > 0$ is a regularization parameter to be prescribed. Formally, $\mathbf{c}^{(1)}_{\lambda^{(1)}}$ is retrieved by solving the normal equation

$$\left[\left(\mathbf{A}^{(11)}\right)^{\mathrm{T}}\mathbf{A}^{(11)} + \lambda^{(1)}\mathbf{I}_{N_s^L}\right]\mathbf{c}^{(1)} = \left(\mathbf{A}^{(11)}\right)^{\mathrm{T}}\mathbf{f}^{(1)}, \tag{29a}$$

namely

$$\mathbf{c}^{(1)}_{\lambda^{(1)}} = \left(\mathbf{A}^{(11)}\right)^{\dagger}\mathbf{f}^{(1)},$$
$$\left(\mathbf{A}^{(11)}\right)^{\dagger} \equiv \left[\left(\mathbf{A}^{(11)}\right)^{\mathrm{T}}\mathbf{A}^{(11)} + \lambda^{(1)}\mathbf{I}_{N_s^L}\right]^{-1}\left(\mathbf{A}^{(11)}\right)^{\mathrm{T}}. \tag{29b}$$

Analogously, the Tikhonov regularized solution, $\mathbf{c}^{(2)}_{\lambda^{(2)}}$, of system (27) is obtained by solving the corresponding normal equation

$$\left[\left(\mathbf{A}^{(22)}\right)^{\mathrm{T}}\mathbf{A}^{(22)} + \lambda^{(2)}\mathbf{I}_{2N_s^E}\right]\mathbf{c}^{(2)} = \left(\mathbf{A}^{(22)}\right)^{\mathrm{T}}\left[\mathbf{f}^{(2)} - \mathbf{A}^{(21)}\mathbf{c}^{(1)}_{\lambda^{(1)}}\right], \tag{30a}$$

namely

$$\mathbf{c}^{(2)}_{\lambda^{(2)}} = \left(\mathbf{A}^{(22)}\right)^{\dagger}\left[\mathbf{f}^{(2)} - \mathbf{A}^{(21)}\mathbf{c}^{(1)}_{\lambda^{(1)}}\right],$$
$$\left(\mathbf{A}^{(22)}\right)^{\dagger} \equiv \left[\left(\mathbf{A}^{(22)}\right)^{\mathrm{T}}\mathbf{A}^{(22)} + \lambda^{(2)}\mathbf{I}_{2N_s^E}\right]^{-1}\left(\mathbf{A}^{(22)}\right)^{\mathrm{T}}, \tag{30b}$$

where $\lambda^{(2)} > 0$ is a regularization parameter to be prescribed.

The optimal values $\lambda^{(1)}_{\mathrm{opt}}$ and $\lambda^{(2)}_{opt}$ of the regularization parameters $\lambda^{(1)} > 0$ and $\lambda^{(2)} > 0$, respectively, are chosen according to Hansen's L-curve criterion (Hansen, 1998).

5. Numerical results

We next apply the algorithm described in Section 3 in conjunction with the regularizing MFS–MPS presented in Section 4 to four test problems. More specifically, we solve the inverse problem governed by the partial differential equations (6) and (8), and subject to the Cauchy boundary conditions (11a) and (11b), for an isotropic linear thermoelastic material (copper alloy) characterised by the material constants $G = 4.80 \times 10^{10}\ \mathrm{N/m^2}$, $\nu = 0.34$, $\kappa = 4.01\ \mathrm{W\,m^{-1}\,K^{-1}}$ and $\alpha_{\mathrm{T}} = 16.5 \times 10^{-6}\ ^{\circ}\mathrm{C}^{-1}$.

Example 1. We consider the annular domain $\Omega = \{\mathbf{x} \in \mathbb{R}^2 \,|\, \mathrm{R_{int}} < \|\mathbf{x}\| < \mathrm{R_{out}}\}$, where $\mathrm{R_{int}} = 1.0$ and $\mathrm{R_{out}} = 2.0$, which is bounded by the inner and outer boundaries $\Gamma_{\mathrm{int}} = \{\mathbf{x} \in \mathbb{R}^2 \,|\, \|\mathbf{x}\| = \mathrm{R_{int}}\}$ and $\Gamma_{\mathrm{out}} = \{\mathbf{x} \in \mathbb{R}^2 \,|\, \|\mathbf{x}\| = \mathrm{R_{out}}\}$, respectively. We also assume that the thermoelastic fields associated with the Example 1 correspond to constant inner and outer temperatures, $\mathrm{T_{int}} = 1\ ^{\circ}\mathrm{C}$ and $\mathrm{T_{out}} = 2\ ^{\circ}\mathrm{C}$, as well as constant inner

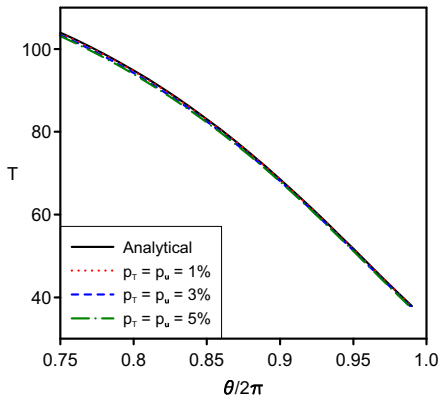

(a) Example 2: $\mathrm{T}|_{\Gamma_2}$

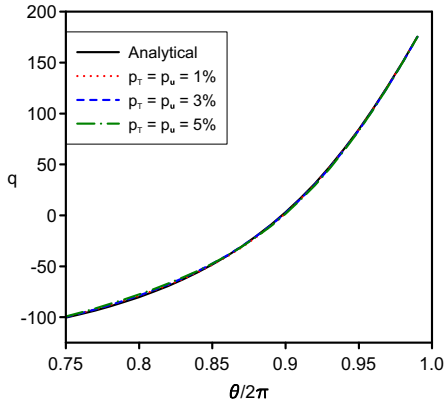

(b) Example 2: $\mathrm{q}|_{\Gamma_2}$

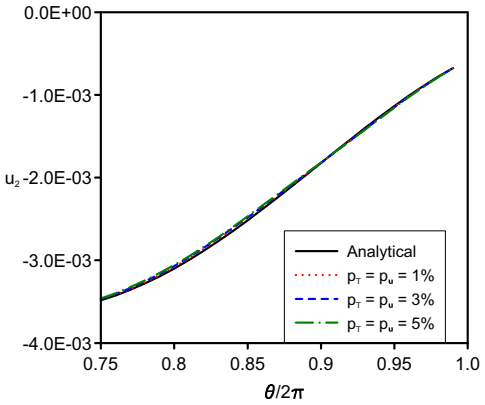

(c) Example 2: $\mathrm{u_2}|_{\Gamma_2}$

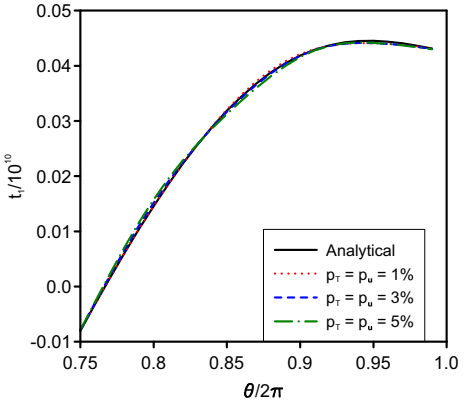

(d) Example 2: $\mathrm{t_1}|_{\Gamma_2}$

Fig. 5. The analytical and numerical (a) temperatures $\mathrm{T}|_{\Gamma_2}$, (b) normal heat fluxes $\mathrm{q}|_{\Gamma_2}$, (c) displacements $\mathrm{u_2}|_{\Gamma_2}$ and tractions (d) $\mathrm{t_1}|_{\Gamma_2}$, obtained using $\mathrm{meas}(\Gamma_1)/\mathrm{meas}(\partial\Omega) = 3/4$, various levels of noise added in $\mathrm{T}|_{\Gamma_1}$ and $\mathrm{u}|_{\Gamma_1}$, for Example 2.

and outer radial pressures, $\sigma_{\text{int}} = 1.0 \times 10^{10}$ N/m^2 and $\sigma_{\text{out}} = 2.0 \times 10^{10}$ N^2, respectively, which describe a plane strain state. The analytical solution of this problem is:

$$\mathrm{T}^{(\text{an})}(\mathbf{x}) = \mathrm{T}_{\text{out}} \frac{\log(\|\mathbf{x}\|/\mathrm{R}_{\text{int}})}{\log(\mathrm{R}_{\text{out}}/\mathrm{R}_{\text{int}})} + \mathrm{T}_{\text{int}} \frac{\log(\mathrm{R}_{\text{out}}/\|\mathbf{x}\|)}{\log(\mathrm{R}_{\text{out}}/\mathrm{R}_{\text{int}})}, \quad \mathbf{x} \in \overline{\Omega}, \tag{31a}$$

$$\mathrm{q}^{(\text{an})}(\mathbf{x}) = -\mathrm{k} \frac{\mathrm{T}_{\text{out}} - \mathrm{T}_{\text{int}}}{\log(\mathrm{R}_{\text{out}}/\mathrm{R}_{\text{int}})} \frac{\mathbf{x} \cdot \mathbf{n}(\mathbf{x})}{\|\mathbf{x}\|^2}, \quad \mathbf{x} \in \partial\Omega, \tag{31b}$$

$$\mathbf{u}^{(\text{an})}(\mathbf{x}) = \left[\frac{\overline{\gamma}}{2}\left(\frac{1-2\overline{\nu}}{1-\overline{\nu}}\right)\frac{\mathrm{T}_{\text{out}} - \mathrm{T}_{\text{int}}}{\log(R_{\text{out}}/R_{\text{int}})}\log\|\mathbf{x}\| + \mathrm{V}\left(\frac{1-\overline{\nu}}{1+\overline{\nu}}\right) - \mathrm{W}\frac{1}{\|\mathbf{x}\|^2}\right]\frac{\mathbf{x}}{2G}, \quad \mathbf{x} \in \overline{\Omega}, \tag{31c}$$

$$\mathbf{t}^{(\text{an})}(\mathbf{x}) = \begin{cases} -\sigma_{\text{out}}\,\mathbf{n}(\mathbf{x}), & \mathbf{x} \in \Gamma_{\text{out}} \equiv \{\mathbf{x} \in \partial\Omega \,|\, \|\mathbf{x}\| = \mathrm{R}_{\text{out}}\}, \\ -\sigma_{\text{int}}\,\mathbf{n}(\mathbf{x}), & \mathbf{x} \in \Gamma_{\text{int}} \equiv \{\mathbf{x} \in \partial\Omega \,|\, \|\mathbf{x}\| = \mathrm{R}_{\text{int}}\}, \end{cases} \tag{31d}$$

where

$$\mathrm{V} \equiv -\frac{\sigma_{\text{out}}^{(\mathrm{H})}\mathrm{R}_{\text{out}}^2 - \sigma_{\text{int}}^{(\mathrm{H})}\mathrm{R}_{\text{int}}^2}{\mathrm{R}_{\text{out}}^2 - \mathrm{R}_{\text{int}}^2}, \quad \mathrm{W} \equiv \frac{\left(\sigma_{\text{out}}^{(\mathrm{H})} - \sigma_{\text{int}}^{(\mathrm{H})}\right)\mathrm{R}_{\text{out}}^2\mathrm{R}_{\text{int}}^2}{\mathrm{R}_{\text{out}}^2 - \mathrm{R}_{\text{int}}^2}, \tag{32a}$$

$$\sigma_{\text{out}}^{(\mathrm{H})} \equiv \sigma_{\text{out}} - \overline{\gamma}\mathrm{T}_{\text{out}} + \frac{\overline{\gamma}}{2}\frac{\mathrm{T}_{\text{out}} - \mathrm{T}_{\text{int}}}{\log(\mathrm{R}_{\text{out}}/\mathrm{R}_{\text{int}})}\left(\frac{1}{1-\overline{\nu}}\log\mathrm{R}_{\text{out}} + 1\right) \tag{32b}$$

and

$$\sigma_{\text{int}}^{(\mathrm{H})} \equiv \sigma_{\text{int}} - \overline{\gamma}\mathrm{T}_{\text{int}} + \frac{\overline{\gamma}}{2}\frac{\mathrm{T}_{\text{out}} - \mathrm{T}_{\text{int}}}{\log(\mathrm{R}_{\text{out}}/\mathrm{R}_{\text{int}})}\left(\frac{1}{1-\overline{\nu}}\log\mathrm{R}_{\text{int}} + 1\right). \tag{32c}$$

Here $\Gamma_1 = \Gamma_{\text{out}}$ and we mention that some preliminary results for Example 1 have been presented in Marin and Karageorghis (2012b).

Example 2. We consider the unit disk $\Omega = \{\mathbf{x} \in \mathbb{R}^2 \,|\, \|\mathbf{x}\| < \mathrm{R}\}$, $\mathrm{R} = 1.0$, and the analytical solution (plane strain state) given by Eqs. (14a), (14b) and (15a)–(15c), where $\mathrm{K} = 1, \mathbf{x}^{(1)} = (2.0, 1.0)$ and $\mathrm{T}_1 = 100\,^\circ$C. Here, we consider $\Gamma_1 = \{\mathbf{x} \in \mathbb{R}^2 \,|\, \|\mathbf{x}\| = \mathrm{R}, \theta \in [0, \theta_0)\}$, where $\theta = \theta(\mathbf{x})$ is the radial angular polar coordinate associated with the point $\mathbf{x} \in \mathbb{R}^2$ and $\theta_0 \in \{\pi/2, \pi, 3\pi/2\}$.

Example 3. We consider the same geometry as in Example 2, with the analytical solution (plane strain state) given by Eqs. (14a), (14b) and (15a)–(15c), where $\mathrm{K} = 2$, $\mathbf{x}^{(1)} = (2.5, 2.5)$, $\mathbf{x}^{(2)} = (1.0, -4.0)$, $\mathrm{T}_1 = 100\,^\circ$C and $\mathrm{T}_2 = 50\,^\circ$C. Here $\Gamma_1 = \{\mathbf{x} \in \mathbb{R}^2 \,|\, \|\mathbf{x}\| = \mathrm{R},\ \theta \in [0, \theta_0)\}$ and $\theta_0 = 3\pi/2$.

Example 4. We consider the square $\Omega = (-1, 1) \times (-1, 1)$, with the analytical solution (plane strain state) given by Eqs. (14a), (14b) and (15a)–(15c), where $\mathrm{K} = 1$, $\mathbf{x}^{(1)} = (2.5, 2.5)$ and $\mathrm{T}_1 = 100\,^\circ$C. Here, we consider $\Gamma_1 = (-1, 1) \times \{\pm 1\} \cup \{1\} \times [-1, 1]$.

In all four examples, we have taken $\mathrm{N}_{\mathrm{c}}^{\mathrm{L}} = \mathrm{N}_{\mathrm{c}}^{\mathrm{E}} = \mathrm{N}$ uniformly distributed collocation points on Γ_1, as well as $\mathrm{N}_{\mathrm{s}}^{\mathrm{L}} = \mathrm{N}_{\mathrm{s}}^{\mathrm{E}} = \mathrm{M}$ uniformly distributed singularities associated with both the over- and under-specified boundaries Γ_1 and Γ_2, respectively, which are preassigned and kept fixed throughout the solution process (i.e. the

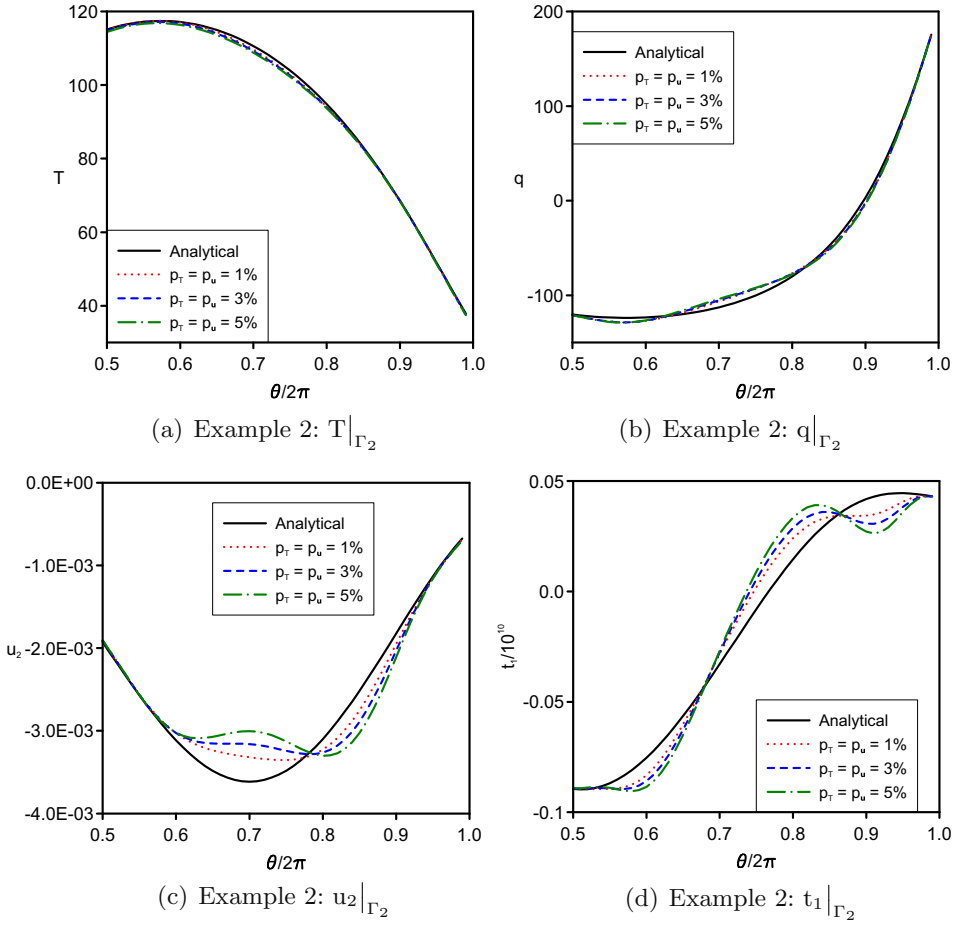

(a) Example 2: $\mathrm{T}\big|_{\Gamma_2}$ (b) Example 2: $\mathrm{q}\big|_{\Gamma_2}$

(c) Example 2: $\mathrm{u}_2\big|_{\Gamma_2}$ (d) Example 2: $\mathrm{t}_1\big|_{\Gamma_2}$

Fig. 6. The analytical and numerical (a) temperatures $\mathrm{T}|_{\Gamma_2}$, (b) normal heat fluxes $\mathrm{q}|_{\Gamma_2}$, (c) displacements $\mathrm{u}_2|_{\Gamma_2}$ and tractions (d) $\mathrm{t}_1|_{\Gamma_2}$, obtained using $\text{meas}(\Gamma_1)/\text{meas}(\partial\Omega) = 1/2$, various levels of noise added in $\mathrm{T}|_{\Gamma_1}$ and $\mathrm{u}|_{\Gamma_1}$, for Example 2.

so-called *static* MFS approach has been employed) on a pseudo-boundary $\partial\widetilde{\Omega}$ of a similar shape to that of $\partial\Omega$ such that $\mathrm{dist}\left(\partial\widetilde{\Omega},\partial\Omega\right)$ is a fixed constant, see e.g. Gorzelańczyk and Kołodziej (2008). According to the notations used in Section 4, the corresponding MFS parameters have been set as follows:

(i) Example 1: $N=56$ on Γ_1, $M_{out}=56$ and $M_{int}=28$ on $\widetilde{\Gamma}_{out}=\{\mathbf{x}\in\mathbb{R}^2\,|\,\|\mathbf{x}\|=R_{out}+d_1\}$ and $\widetilde{\Gamma}_{int}=\{\mathbf{x}\in\mathbb{R}^2\,|\,\|\mathbf{x}\|=R_{int}-d_2\}$, respectively, such that $M=M_{out}+M_{int}$, where $\partial\widetilde{\Omega}=\widetilde{\Gamma}_{out}\cup\widetilde{\Gamma}_{int}$, $d_1=1.0$ and $d_2=0.3$.

(ii) Examples 2 and 3: $M=48$ on $\partial\widetilde{\Omega}=\{\mathbf{x}\in\mathbb{R}^2\,|\,\|\mathbf{x}\|=R+d\}$, where $d=0.5$ and $N=k(M/4)$ on Γ_1 for $\theta_0=k(\pi/2)$ with $k\in\{1,2,3\}$.

(iii) Example 4: $M=56$ on $\partial\widetilde{\Omega}=[-(1+d),(1+d)]\times\{\pm(1+d)\}\cup\{\pm(1+d)\}\times[-(1+d),(1+d)]$, where $d=1.0$ and $N=3(M/4)$ on Γ_1.

We consider the Cauchy problem given by Eqs. (6), (8) and (11) with the over- and under specified boundaries Γ_1 and $\Gamma_2=\partial\Omega\setminus\overline{\Gamma}_1$, respectively, and perturbed boundary temperature and displacements on Γ_1. More precisely, the boundary temperature $T|_{\Gamma_1}=T^{(an)}|_{\Gamma_1}$ and displacements $u_j|_{\Gamma_1}=u_j^{(an)}|_{\Gamma_1}$, $j=1,2$, on the over-specified boundary have been perturbed as

$$\widetilde{T}^{\varepsilon}|_{\Gamma_1}=T|_{\Gamma_1}+\delta T,\quad \delta T=\texttt{G05DDF}(0,\sigma_T),\qquad \sigma_T=\max_{\Gamma_1}|T|\times(p_T/100) \tag{33a}$$

and

$$\widetilde{u}_j^{\varepsilon}|_{\Gamma_1}=u_j|_{\Gamma_1}+\delta u_j,\quad \delta u_j=\texttt{G05DDF}(0,\sigma_{u_j}),\qquad \sigma_{u_j}=\max_{\Gamma_1}|u_j|\times(p_u/100),\quad j=1,2, \tag{33b}$$

respectively. Here δT and δu_j are Gaussian random variables with mean zero and standard deviations σ_T and σ_{u_j}, respectively, generated by the NAG subroutine G05DDF (Numerical Algorithms Group Library Mark 21, 2007), while p_T and p_u are the percentages of additive noise included in the input boundary temperature $T|_{\Gamma_1}$ and displacements $u_j|_{\Gamma_1}$, $j=1,2$, respectively, in order to simulate the inherent measurement errors. It should be mentioned that, for the inverse problems with noisy boundary data considered herein, the accuracy of the numerical results was found to be quite insensitive with respect to the location of the pseudo-boundary.

Figs. 1(a) and (b) present the numerical results for the temperature and normal heat flux, respectively, on the under-specified boundary Γ_2, obtained by solving the thermal Cauchy problem (6) and (11a), for Example 1, using the proposed Tikhonov regularization method, Hansen's L-curve criterion and $p_T=p_u=1\%,3\%,5\%$, in comparison with their corresponding analytical values. The numerical solutions for the temperature and normal heat flux on Γ_2 are stable approximations of their corresponding exact solutions, free of unbounded and rapid oscillations, and they converge to the exact solutions as the level of noise decreases.

In order to assess the accuracy and convergence of the proposed MFS–MPS approach, for any real-valued function $f:\Gamma_2\longrightarrow\mathbb{R}$ and any set of points $\{x^{(n)}\}_{n=1}^{N_2}\subset\Gamma_2$, we define the corresponding *root mean square* (RMS) *error* of f on Γ_2 and the *relative RMS error* of f on Γ_2 by

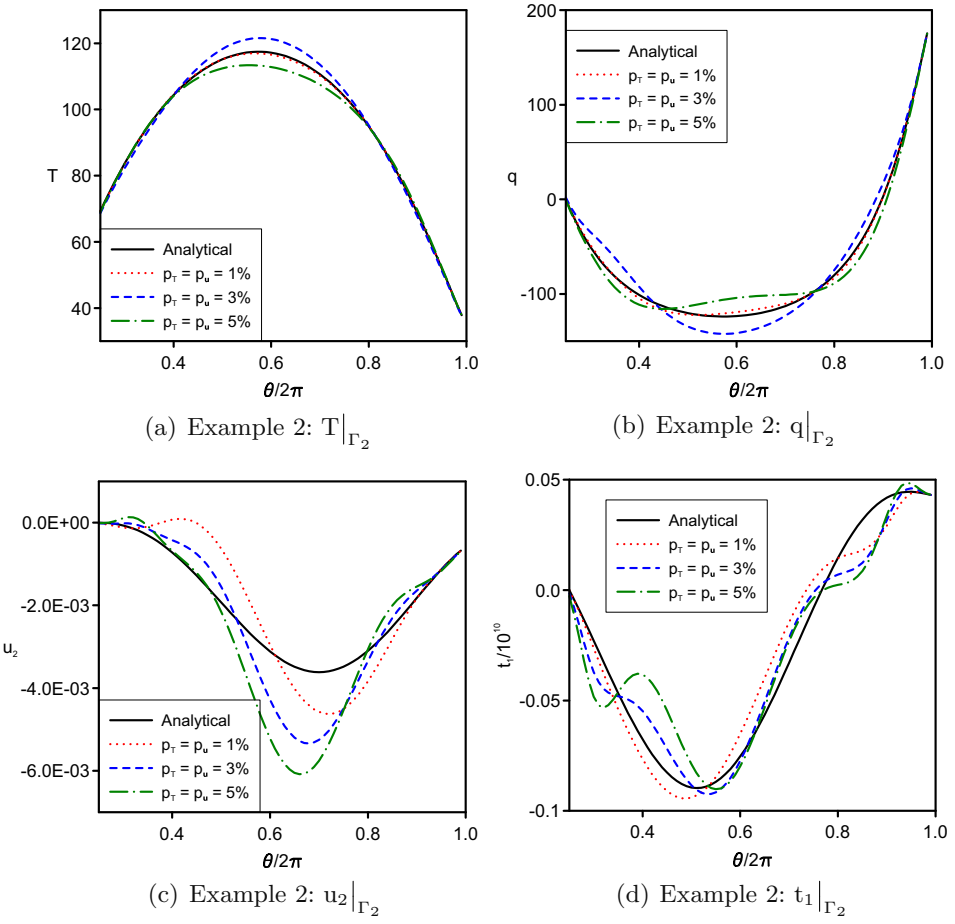

(a) Example 2: $T|_{\Gamma_2}$ (b) Example 2: $q|_{\Gamma_2}$

(c) Example 2: $u_2|_{\Gamma_2}$ (d) Example 2: $t_1|_{\Gamma_2}$

Fig. 7. The analytical and numerical (a) temperatures $T|_{\Gamma_2}$, (b) normal heat fluxes $q|_{\Gamma_2}$, (c) displacements $u_2|_{\Gamma_2}$ and tractions (d) $t_1|_{\Gamma_2}$, obtained using $\mathrm{meas}(\Gamma_1)/\mathrm{meas}(\partial\Omega)=1/4$, various levels of noise added in $T|_{\Gamma_1}$ and $u|_{\Gamma_1}$, for Example 2.

$$\mathrm{RMS}_{\Gamma_2}(f) = \sqrt{\frac{1}{N_2}\sum_{n=1}^{N_2} f(\mathrm{x}^{(n)})^2} \tag{34a}$$

and

$$\mathrm{E}_f = \frac{\mathrm{RMS}_{\Gamma_2}(f^{(num)} - f)}{RMS_{\Gamma_2}(f)}, \tag{34b}$$

respectively, where $f^{(\mathrm{num})}(\mathrm{x})$ denotes an approximate numerical value for $f(\mathrm{x}), \mathrm{x} \in \Gamma_2$.

The corresponding relative RMS errors (34b) for the boundary temperature and normal heat flux on Γ_2 are presented in Figs. 2(a) and (b), respectively. For each level of noise added to the prescribed boundary temperature $\mathrm{T}|_{\Gamma_1}$ and displacements $\mathrm{u}_j|_{\Gamma_1}, j = 1, 2$, the numerical results for the normal heat flux on Γ_2 are, as expected, more inaccurate than those retrieved for the corresponding boundary temperature, i.e. $\mathrm{E}_\mathrm{T} < \mathrm{E}_\mathrm{q}$ for all $\mathrm{p}_\mathrm{T} = \mathrm{p}_\mathrm{u} \in \{1\%, 3\%, 5\%\}$. Moreover, Figs. 2(a) and (b) also show the convergence of the reconstructed boundary temperature and normal heat flux on Γ_2 to their corresponding exact values as the level of noise decreases. The L-curves associated with the Tikhonov regularized solution $\mathrm{c}^{(1)}_{\lambda^{(1)}}$ of system (19), obtained for Example 1 with $\mathrm{p}_\mathrm{T} = \mathrm{p}_\mathrm{u} \in \{1\%, 3\%, 5\%\}$, are shown in Fig. 2(c). By comparing Figs. 2(a)–(c), one can conclude that Hansen's L-curve criterion provides an excellent estimation of the minimum attained by the relative RMS errors E_T and E_q and hence this criterion is a suitable tool for the selection of the optimal regularization parameter $\lambda^{(1)}_{\mathrm{opt}}$.

Stable and convergent numerical results have also been obtained for the displacement and traction vectors on the under-specified boundary Γ_2 for Example 1 for $\mathrm{p}_\mathrm{T} = \mathrm{p}_\mathrm{u} = 1\%, 3\%, 5\%$. These boundary data reconstructions for $\mathrm{u}_1|_{\Gamma_2}, \mathrm{u}_2|_{\Gamma_2}, \mathrm{t}_1|_{\Gamma_2}$ and $\mathrm{t}_2|_{\Gamma_2}$ are presented in Figs. 3(a)–(d), respectively, together with their corresponding exact values. The relative RMS error (34b) of the boundary displacement and traction vectors on Γ_2, as well as the L-curves associated with the Tikhonov regularized solution, $\mathrm{c}^{(2)}_{\lambda^{(2)}}$, of system (27), are shown in Figs. 4(a)–(c), respectively.

Similar conclusions regarding the convergence, stability and accuracy of the proposed method can be drawn if one considers the Cauchy problem (6), (8) and (11) with perturbed temperatures and displacements on Γ_1 in the simply connected domain represented by the unit disk of Example 2. Figs. 5–7 present the analytical and numerical results for the boundary temperature, normal heat flux, x_2-component of the displacement vector and x_1-component of the traction vector data on Γ_2, retrieved in three situations, namely for $\mathrm{meas}(\Gamma_1)/\mathrm{meas}(\partial\Omega) \in \{3/4, 1/2, 1/4\}$. Although the numerical results retrieved for both the thermal and the mechanical fields on Γ_2 are convergent and stable with respect to decreasing the amount of noise added to the Cauchy data in all cases analysed for Example 2, prescribing noisy boundary data on a small accessible boundary (i.e. for $\mathrm{meas}(\Gamma_1)/\mathrm{meas}(\partial\Omega) = 1/4$ or, equivalently, $\mathrm{meas}(\Gamma_1)/\mathrm{meas}(\Gamma_2) < 1$) yields inaccurate numerical results especially for the displacement and traction vectors, see Figs. 7(a)–(d).

Finally, we analyse the numerical results obtained using the proposed algorithm for a more complicated analytical solution in a simply connected domain with a smooth boundary as given by

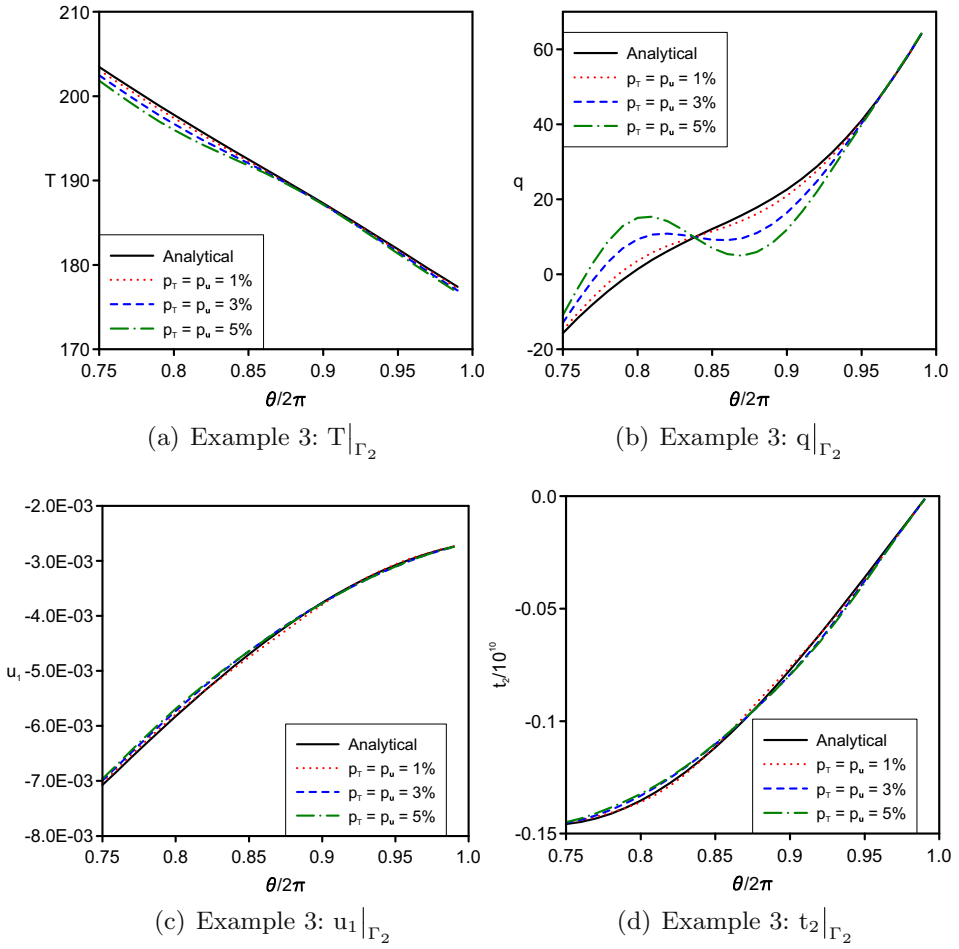

(a) Example 3: $\mathrm{T}\big|_{\Gamma_2}$ (b) Example 3: $\mathrm{q}\big|_{\Gamma_2}$

(c) Example 3: $\mathrm{u}_1\big|_{\Gamma_2}$ (d) Example 3: $\mathrm{t}_2\big|_{\Gamma_2}$

Fig. 8. The analytical and numerical (a) temperatures $\mathrm{T}|_{\Gamma_2}$, (b) normal heat fluxes $\mathrm{q}|_{\Gamma_2}$, (c) displacements $\mathrm{u}_1|_{\Gamma_2}$ and (d) tractions $\mathrm{t}_2|_{\Gamma_2}$, obtained using various levels of noise added in $\mathrm{T}|_{\Gamma_1}$ and $\mathrm{u}|_{\Gamma_1}$, for Example 3.

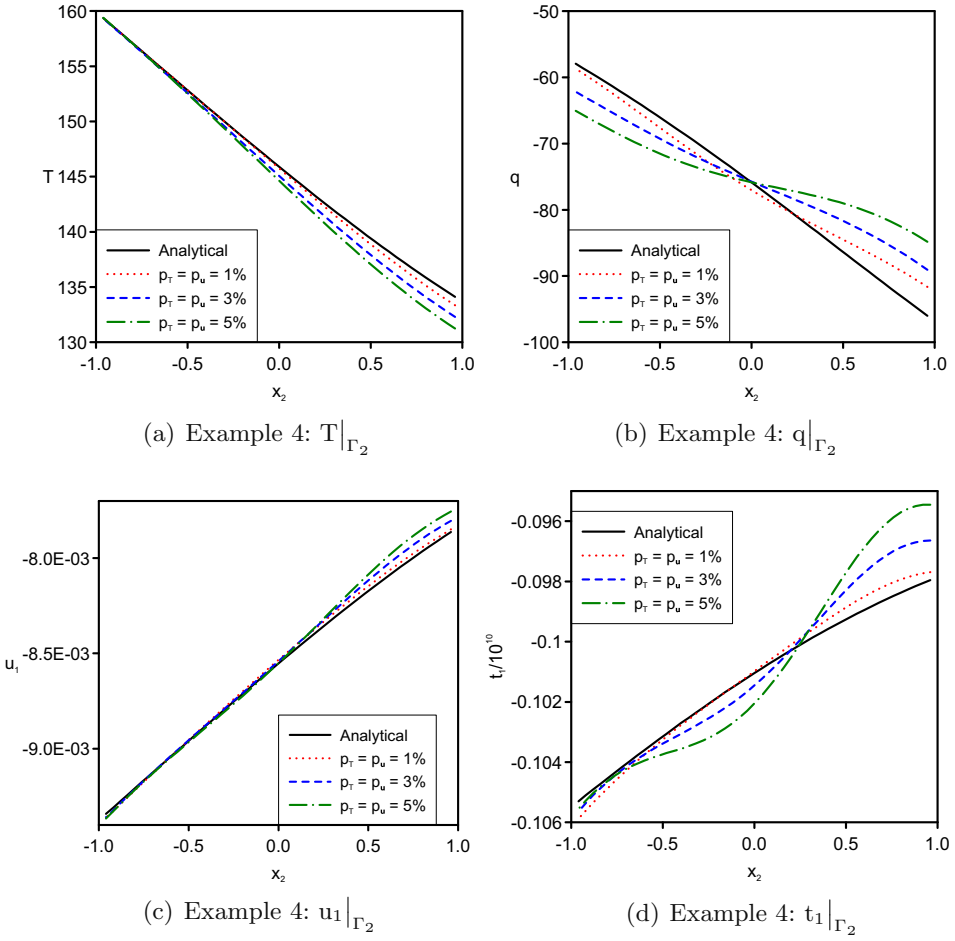

(a) Example 4: $T|_{\Gamma_2}$ (b) Example 4: $q|_{\Gamma_2}$

(c) Example 4: $u_1|_{\Gamma_2}$ (d) Example 4: $t_1|_{\Gamma_2}$

Fig. 9. The analytical and numerical (a) temperatures $T|_{\Gamma_2}$, (b) normal heat fluxes $q|_{\Gamma_2}$, (c) displacements $u_1|_{\Gamma_2}$ and (d) tractions $t_1|_{\Gamma_2}$, obtained using various levels of noise added in $T|_{\Gamma_1}$ and $u|_{\Gamma_1}$, for Example 4.

Example 3, as well as in a simply connected domain with a piecewise smooth boundary such as the square considered in Example 4. The analytical and numerical results for the unknown thermal and mechanical boundary data, obtained using the proposed method, Hansen's L-curve criterion and $p_T = p_u = 1\%, 3\%, 5\%$, for Examples 3 and 4, are presented in Figs. 8 and 9, respectively.

Overall, from the four examples investigated, we can conclude that the proposed method provides accurate, convergent and stable numerical approximations with respect to decreasing the level of noise added to the Cauchy data, for the unknown thermal and mechanical data.

6. Conclusions

In this work, we applied the MFS in conjunction with the MPS for the numerical solution of the inverse Cauchy problem in two-dimensional linear isotropic thermoelasticity. The key idea in this approach is the construction of a particular solution of the non-homogeneous equations of equilibrium which only depends on the MFS approximation of the boundary value problem for the heat conduction equation. The inverse problem was regularized/stabilised via the Tikhonov regularization method (Tikhonov and Arsenin, 1986), while the optimal value of the regularization parameter was selected by employing Hansen's L-curve criterion (Hansen, 1998). The accuracy, convergence and stability properties of the proposed MFS–MPS–Tikhonov regularization method were investigated by considering four numerical examples in simply and doubly connected domains with either a smooth or a piecewise smooth boundary. Future work is related to the development of fast MFS–MPS algorithms for inverse problems in two-dimensional isotropic thermoelasticity (Karageorghis and Marin, 2013), as well as the application of the proposed MFS–MPS procedure for the stable numerical solution of inverse boundary value problems in three-dimensional isotropic thermoelasticity.

Acknowledgements

The financial support received from the Romanian National Authority for Scientific Research (CNCS-UEFISCDI), project number PN-II-ID-PCE-2011-3-0521, is gratefully acknowledged.

References

Aliabadi, M.H., 2002. The Boundary Element Method. Applications in Solids and Structures, vol. 2.. John Wiley & Sons, London.
Chen, C.W., Young, D.L., Tsai, C.C., Murugesan, K., 2005. The method of fundamental solutions for inverse 2D Stokes problems. Computational Mechanics 37, 2–14.
Cheng, A.H.–D., Chen, C.S., Golberg, M.A., Rashed, Y.F., 2001. BEM for thermoelasticity and elasticity with body force – a revisit. Engineering Analysis with Boundary Elements 25, 377–387.
Ciałkowski, M.J., Frąckowiak, A., 2002. Solution of the stationary 2D inverse heat conduction problem by Trefftz method. Journal of Thermal Science 11, 148–162.
Ciałkowski, M., Grysa, K., 2010. Trefftz method in solving the inverse problems. Journal of Inverse and Ill-Posed Problems 18, 595–616.
Ciałkowski, M.J., Frąckowiak, A., Grysa, K., 2007a. Physical regularization for inverse problems of stationary heat conduction. Journal of Inverse and Ill-Posed Problems 15, 347–364.
Ciałkowski, M.J., Frąckowiak, A., Grysa, K., 2007b. Solution of a stationary inverse heat conduction problem by means of Trefftz non-continuous method. International Journal of Heat and Mass Transfer 50, 2170–2181.

Dennis, B.H., Dulikravich, G.S., 1998. Elsevier Science, BV, UK, pp. 61–70.
Dennis, B.H., Dulikravich, G.S., 1999. A finite element formulation for the detection of boundary conditions in elasticity and heat conduction. In: Tanaka, M., Dulikravich, G.S. (Eds.), Inverse Problems in Engineering Mechanics. Elsevier Science BV, UK, pp. 61–70.
Dong, C.F., Sun, F.Y., Meng, B.Q., 2007. A method of fundamental solutions for inverse heat conduction problems in an anisotropic medium. Engineering Analysis with Boundary Elements 31, 75–82.
Fairweather, G., Karageorghis, A., 1998. The method of fundamental solutions for elliptic boundary value problems. Advances in Computational Mathematics 9, 69–95.
Fairweather, G., Karageorghis, A., Martin, P.A., 2003. The method of fundamental solutions for scattering and radiation problems. Engineering Analysis with Boundary Elements 27, 759–769.
Golberg, M.A., Chen, C.S., 1999. The method of fundamental solutions for potential, Helmholtz and diffusion problems. In: Boundary Integral Methods: Numerical and Mathematical Aspects. In: Golberg, M.A. (Ed.), . Computational Engineering, vol. 1. WIT Press/Computational Mechanics Publications, Boston, MA, pp. 103–176.
Gorzelańczyk, P., Kołodziej, J.A., 2008. Some remarks concerning the shape of the shape contour with application of the method of fundamental solutions to elastic torsion of prismatic rods. Engineering Analysis with Boundary Elements 32, 64–75.
Hadamard, J., 1923. Lectures on Cauchy's Problem in Linear Partial Differential Equations. Yale University Press, Hew Haven.
Hansen, P.C., 1998. Rank-Deficient and Discrete Ill-Posed Problems: Numerical Aspects of Linear Inversion. SIAM, Philadelphia.
Henry Jr., D.P., Banerjee, P.K., 1988. A new boundary element formulation for two- and three-dimensional thermoelasticity using particular integrals. International Journal for Numerical Methods in Engineering 26, 2061–2077.
Hon, Y.C., Wei, T., 2004. A fundamental solution method for inverse heat conduction problems. Engineering Analysis with Boundary Elements 28, 489–495.
Hon, Y.C., Wei, T., 2005. The method of fundamental solutions for solving multidimensional heat conduction problems. CMES: Computer Modeling in Engineering & Sciences 13, 219–228.
Jin, B.T., Zheng, Y., 2006. A meshless method for some inverse problems associated with the Helmholtz equation. Computer Methods in Applied Mechanics and Engineering 195, 2270–2280.
Kamiya, N., Aikawa, Y., Kawaguchi, K., 1994. An adaptive boundary element scheme for steady thermoelastic analysis. Computer Methods in Applied Mechanics and Engineering 119, 311–324.
Karageorghis, A., Marin, L., 2013. Efficient MFS algorithms for problems in thermoelasticity. Journal of Scientific Computing 56, 96–121.
Karageorghis, A., Smyrlis, Y.-S., 2007. Matrix decomposition MFS algorithms for elasticity and thermo-elasticity problems in axisymmetric domains. Journal of Computational and Applied Mathematics 206, 774–795.
Karageorghis, A., Lesnic, D., Marin, L., 2011. A survey of applications of the MFS to inverse problems. Inverse Problems in Science and Engineering 19, 309–336.
Karageorghis, A., Lesnic, D., Marin, L., 2013. Regularized Trefftz collocation method for void detection in two-dimensional steady-state heat conduction problems. Inverse Problems in Science and Engineering. doi: http://dx.doi.org/10.1080/17415977.2013.788172.
Karaś, M.S., Zieliński, A.P., 2008. Boundary-values recovery by Trefftz approach in structural inverse problems. Communications in Numerical Methods in Engineering 24, 605–625.
Kita, E., Kamiya, N., 1995. Trefftz method an overview. Advances in Engineering Software 24, 3–12.
Liu, C.S., 2008a. A modified collocation Trefftz method for the inverse Cauchy problem of Laplace equation. Engineering Analysis with Boundary Elements 32, 778–785.
Liu, C.S., 2008b. A highly accurate MCTM for inverse Cauchy problems of Laplace equation in arbitrary plane domains. CMES: Computer Modeling in Engineering & Sciences 35, 91–111.
Marin, L., 2005a. A meshless method for solving the Cauchy problem in three-dimensional elastostatics. Computers & Mathematics with Applications 50, 73–92.
Marin, L., 2005b. Numerical solution of the Cauchy problem for steady-state heat transfer in two-dimensional functionally graded materials. International Journal of Solids and Structures 42, 4338–4351.
Marin, L., 2005c. A meshless method for the numerical solution of the Cauchy problem associated with three-dimensional Helmholtz-type equations. Applied Mathematics and Computation 165, 355–374.
Marin, L., 2008. The method of fundamental solutions for inverse problems associated with the steady-state heat conduction in the presence of sources. CMES: Computer Modeling in Engineering & Sciences 30, 99–122.
Marin, L., Karageorghis, A., 2012a. MFS-based solution to two-dimensional linear thermoelasticity problems. In: Brebbia, C.A., Poljak, D. (Eds.), Boundary Elements and other Mesh Reduction Methods XXXIV (BEM/MRM 2012). WIT Press, Southampton, UK, pp. 39–49.
Marin, L., Karageorghis, A., 2012b. MFS solution of inverse boundary value problems in two-dimensional linear thermoelasticity. In: Aliabadi, M.H., Prochazka, P. (Eds.), Advances in Boundary Element Techniques XIII: International Conference on Boundary Element and Meshless Techniques XII. EC Ltd., UK, pp. 141–146.
Marin, L., Karageorghis, A., 2013. The MFS–MPS for two-dimensional steady-state thermoelasticity problems. Engineering Analysis with Boundary Elements 37, 1004–1020.
Marin, L., Lesnic, D., 2004. The method of fundamental solutions for the Cauchy problem in two-dimensional linear elasticity. International Journal of Solids and Structures 41, 3425–3438.
Marin, L., Lesnic, D., 2005a. The method of fundamental solutions for the Cauchy problem associated with two-dimensional Helmholtz-type equations. Computers & Structures 83, 267–278.
Marin, L., Lesnic, D., 2005b. The method of fundamental solutions for inverse boundary value problems associated with the two-dimensional biharmonic equation. Mathematical and Computers in Modelling 42, 261–278.
Mathon, R., Johnston, R.L., 1977. The approximate solution of elliptic boundary value problems by fundamental solutions. SIAM Journal on Numerical Analysis 14, 638–650.
Nowacki, W., 1986. Thermoelasticity. Pergamon Press, Oxford.
Numerical Algorithms Group Library Mark 21, 2007. NAG(UK) Ltd., Wilkinson House, Jordan Hill Road, Oxford, UK.
Partridge, P.W., Brebbia, C.A., Wrobel, L.C., 1992. The Dual Reciprocity Boundary Element Method. Computational Mechanics Publications, Southampton.
Rizzo, F.J., Shippy, D.J., 1977. An advanced boundary integral equation method for three-dimensional thermoelasticity. International Journal for Numerical Methods in Engineering 11, 1753–1768.
Rizzo, F.J., Shippy, D.J., 1979. The boundary elemcnt method in thermoelasticity. In: Banerjee, P.K., Butterfield, R. (Eds.), Developments in Boundary Element Methods – I. Applied Science Publishers, London.
Sladek, V., Sladek, J., 1983. Boundary integral equation in thermoelasticity. Part I: General analysis. Applied Mathematical Modelling 7, 413–418.
Sladek, V., Sladek, J., 1984. Boundary integral equation in thermoelasticity. Part III: Uncoupled thermoelasticity. Applied Mathematical Modelling 8, 413–418.
Sladek, J., Sladek, V., Atluri, S.N., 2001. A pure contour formulation for the meshless local boundary integral equation method in thermoelasticity. CMES: Computer Modeling in Engineering and Science 2, 423–433.
Tikhonov, A.N., Arsenin, V.Y., 1986. Methods for Solving Ill-Posed Problems. Nauka, Moscow.
Trefftz, E., 1926. Ein Gegenstück zum Ritzschen Verfahren. In: Verhandlungen des 2. Internationalen Kongresses für Technische Mechanik, Zürich, Switzerland, pp. 131–137.
Tsai, C.C., 2009. The method of fundamental solutions with dual reciprocity for three-dimensional thermoelasticity under arbitrary forces. International Journal for Computer-Aided Engineering and Software 26, 229–244.
Wei, T., Hon, Y.C., Ling, L., 2007. Method of fundamental solutions with regularization techniques for Cauchy problems of elliptic operators. Engineering Analysis with Boundary Elements 31, 373–385.
Wróblewski, A., Zieliński, A.P., 2006. Structural inverse problems solved by the T-element approach. Computer Assisted Mechanics and Engineering Science 13, 473–480.